

SPATIAL DISTRIBUTION OF PORES IN TRANSLUCENT ALUMINA STUDIED
WITH A CONFOCAL SCANNING LASER MICROSCOPE

Lars M. Karlsson¹, Anders Liljeborg²

¹Materials Technology, Royal Institute of Technology,
S-100 44 Stockholm, Sweden

²Physics IV, Royal Institute of Technology,
S-100 44 Stockholm, Sweden

ABSTRACT

The spatial distribution of pores in translucent alumina was studied with a confocal scanning laser microscope, computer based image analysis, and spatial statistical methods. The analysis suggested that the pore centroids were clustered within a range up to about 15 μm .

Key words: alumina, confocal microscopy, pores, spatial distribution, stereology.

INTRODUCTION

"Are particles clustered within specific regions of space, or can they be regarded as randomly distributed?" is a question often asked by scientists in various disciplines. The arrangement of particles in space can be analysed from the corresponding spatial point pattern, that is, a set of points in space. A point pattern may be obtained by associating a unique point with each particle. There are techniques for analysing two-dimensional point patterns (see e.g. Diggle, 1983), as well as three-dimensional (3-D) patterns (Baddeley et al., 1987; König et al., 1991). The 3-D arrangement of particles has previously been studied in biological and medical applications by Baddeley et al. (1987) and König et al. (1991). The purpose of this paper is to present a similar study, but applied to an example from the field of materials science; namely, pores in translucent alumina.

For translucent or transparent materials, the confocal scanning laser microscope (CSLM) offers unique possibilities to study particles directly in 3-D without the requirement to physically sectioning the specimen. By moving the focal plane of a CSLM up or down through the specimen, a stack of thin ($\sim 1 \mu\text{m}$) optical sections was obtained. A 3-D image of the pores was produced with computer based image analysis from this stack of sections. The coordinates of the pore centroids were calculated by computer based image analysis, and the spatial distribution of the centroids was analysed with 3-D statistical methods. The analysis suggested that the pore centroids were clustered within a range up to about 15 μm .

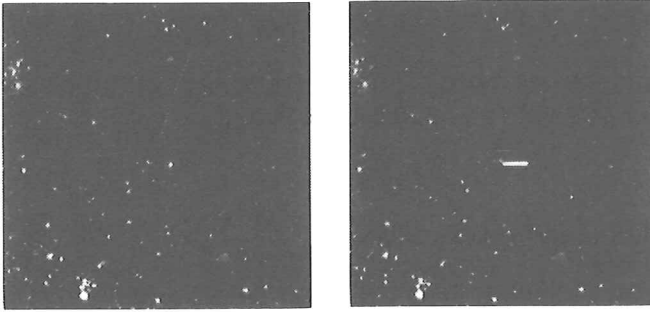


Figure 1: Stereo-pair micrograph showing pores in translucent alumina.—A stack of optical sections was projected on a plane along two directions which were 5° apart. The oblong object at the centre is an internal reflection in the microscope. The side length of each micrograph is about $100\ \mu\text{m}$.

MATERIAL AND EXPERIMENTAL METHODS

The material used in this study was a highly translucent polycrystalline alumina ceramic (brand name Lucalox). It was available as a 4 cm long bar with quadratic cross section of $12 \times 12\ \text{mm}$. A block about $1\ \text{cm}^3$ was cut off from the bar, and four sides of the block (perpendicular to the cut face) were ground and polished following conventional procedures.

The confocal laser microscope scanner PHOIBOS (Carlsson and Liljeborg, 1989) developed at Physics IV, the Royal Institute of Technology, Stockholm (Sweden), was used to record serial optical sections. The specimen was illuminated with visible light (514 nm) from an argon laser, and the reflected light from the specimen was detected. A $\lambda/4$ retardation plate was introduced in the microscope optics as well as a polarizer in front of the detector. These measures almost removed a strong and unpleasant retro-reflection of the laser beam for certain scanning angles. However, a small reflection at the centre of the field of view still remained. The $100\times$ oil immersion objective ($\text{NA}=1.3$) was used.

A stack of serial optical sections (making a 'reference brick') was automatically recorded. The focus setting of the microscope was computer-controlled. From an initial position just below the surface of the specimen, 70 sections separated by steps of $1\ \mu\text{m}$ from one another were recorded. Each section was digitally recorded as 512×512 picture elements (pixels) with 256 grey levels. Pore profiles were visible as bright spots. With the pixel size used ($0.2\ \mu\text{m}/\text{pixel}$) each section corresponded to an area of $102 \times 102\ \mu\text{m}^2$ at the specimen scale. Each reference brick therefore had a total volume of $728\ 280\ \mu\text{m}^3$ ($102 \times 102 \times 70\ \mu\text{m}$). Eight independent bricks of equal size were recorded.

A 3×3 smoothing operation was applied to each digitised section to reduce noise due to the distribution of photons in the detected light. The voxels belonging to pores were computed by thresholding, and the coordinates of the centroids were calculated and stored on disc. Computer based image analysis was used for this purpose. Also 3-D images at different angles could be computed for visualisation (see Fig. 1).

The associated point rule (Miles, 1978) was used to cope with edge effects in bounded

blocks of material. A single point—here the pore centroid—was associated with each pore. Only points inside a 'counting brick', that is, a smaller brick positioned inside the reference brick, were considered. A 'guard volume', large enough to encompass the largest pore, must exist outside the counting brick. The width of the guard volume surrounding the six faces of the counting brick ranged from 3 to 13 μm . The volume of the counting brick was $477\,144\,\mu\text{m}^3$ ($94 \times 94 \times 54\,\mu\text{m}$).

The pore centroids that were inside the eight counting bricks constituted the final sample of the observed pores. Statistical analysis (see next section) was applied to these points.

STATISTICAL METHODS

A set of points irregularly distributed within a region of space is called a spatial point pattern. Any random mechanism which generates such points is called a spatial point process. A simple summary of a spatial point pattern is provided by the so called K -function (Diggle, 1983; Baddeley et al., 1987; König et al., 1991). It is a measure of the expected number of points to be found within a distance r from a typical point of a point pattern, excluding the latter point. Thus:

$$K(r) = \frac{E(\text{number of points within distance } r \text{ of an arbitrary point}) - 1}{N_V} \quad (1)$$

where $E(\cdot)$ denotes expectation (mean) over all possible outcomes of the random point pattern and N_V is the number of points per unit reference volume. The Poisson point process (see e.g. König et al., 1991), is a model for 'complete spatial randomness' of a point pattern. For this process, the expected number of points found within a sphere of radius r is simply N_V times the volume of the sphere. The K -function for the Poisson process is thus $K_{\text{Poi}}(r) = 4\pi r^3/3$, which may be used as a reference model. If $K(r) > 4\pi r^3/3$ for a range of r it is interpreted as clustering (attraction) of points. Conversely, if $K(r) < 4\pi r^3/3$ it means inhibition (repulsion) between points, or that they are arranged in a systematic pattern. An estimator $\text{est}K(r)$ of the K -function is:

$$\text{est}K(r) = \frac{\text{vol}(B)}{n^2} \sum_{\substack{d_{ij} \leq r \\ i \neq j}} w_{ij}^{-1} \quad (2)$$

where n is the number of points in a point pattern within the 3-D region B of volume $\text{vol}(B)$; d_{ij} is the distance between the i th and the j th point; and w_{ij} is an edge-correction factor, equal to the proportion of the surface area of a sphere centred at the i th point and having radius d_{ij} , which lies within B . In general $w_{ij} \neq w_{ji}$. This estimator is unbiased for sufficiently small r . The algorithm for calculating w_{ij} given in König et al. (1991, Appendix 2) was used in this study.

The L -function (König et al., 1991) is a linearized version of the K -function defined as:

$$L(r) = \left[\frac{3 \cdot K(r)}{4\pi} \right]^{1/3} \quad (3)$$

where $K(r)$ is defined in Eq. 1. For a Poisson point process, $L_{\text{Poi}}(r) = r$, giving a linear function which is convenient for comparison with the estimated L -function from an observed point pattern. If $L(r) > r$ for a range of r , it is interpreted as clustering of

points. If $L(r) < r$ it means inhibition between points, or that they are systematically arranged. An estimator of $L(r)$ is obtained by replacing $K(r)$ in Eq. 3 with the estimator in Eq. 2.

The H-function (König et al., 1991) is the difference between the K -function and the corresponding function for a Poisson point process:

$$H(r) = K(r) - K_{\text{Poi}}(r) \quad (4)$$

It becomes zero if the observed $K(r)$ is the same as that for the Poisson reference model $K_{\text{Poi}}(r)$. An estimator of $H(r)$ is obtained by replacing $K(r)$ in Eq. 4 with the estimator in Eq. 2.

RESULTS

The number of points n counted in the eight counting bricks were: 122, 140, 139, 114, 122, 95, 118, and 97. Each counting brick was of height $h = 54 \mu\text{m}$, base area $a = 8\,836 \mu\text{m}^2$ and volume $V = a \cdot h = 477\,144 \mu\text{m}^3$. An estimate of the number of pores per unit volume N_V was calculated as n/V . The overall mean for the eight bricks was $2.48 \times 10^{-4} \mu\text{m}^{-3}$ with about 5% CE (coefficient of error, i.e., the standard error divided with the mean).

Estimates of $K(r)$ were calculated for each brick according to Eq. 2. These estimates are shown in Fig. 2a together with lower and upper bounds of $K(r)$ from 500 independent simulations of the Poisson point process.

Estimates of $L(r)$ and $H(r)$ were calculated from the estimates of $K(r)$ as suggested by Eqs. 3 and 4, respectively. These estimates are shown together with lower and upper simulation bounds of the corresponding functions in Figs. 2c and 2e.

Overall estimates from the eight bricks of $K(r)$, $L(r)$, and $H(r)$ were calculated as ratio estimators (Baddeley et al., 1987). These estimates are shown together with the corresponding functions of the theoretical Poisson reference model in Figs. 2b, 2d, and 2f.

DISCUSSION

The estimated pore density N_V (overall mean $2.48 \times 10^{-4} \mu\text{m}^{-3}$) was smaller than that reported in Russ et al., 1989 ($7.28 \times 10^{-3} \mu\text{m}^{-3}$). This could be accounted for by a difference in grain size; the material used by Russ et al. was processed to a very fine ($\sim 1.5 \mu\text{m}$) grain diameter, whereas the material used in this study was coarse grained (no quantitative estimation of grain size was done). The pores are generally located at the grain boundaries, thus the difference in pore density between the alumina used in this study and the alumina used by Russ et al.

For small r -values (up to about $15 \mu\text{m}$), the individual estimates from the eight bricks of $K(r)$, $L(r)$, and $H(r)$ lie above or around the corresponding upper simulation bounds (see Figs. 2a, 2c, and 2e). The overall estimates of $K(r)$, $L(r)$, and $H(r)$ are larger than the corresponding functions of the theoretical Poisson reference model (see Figs. 2b, 2d, and 2f). Our conclusion is that the analysis suggests that the pore centroids are clustered within a range up to about $15 \mu\text{m}$, which is clearly shown in Figs. 2c-f.

The overall estimate from the eight bricks was also calculated as an ordinary average, that is, as an arithmetic mean (Baddeley et al., 1987), which was in excellent agreement with the ratio estimator. Generally the ratio estimator is to prefer.

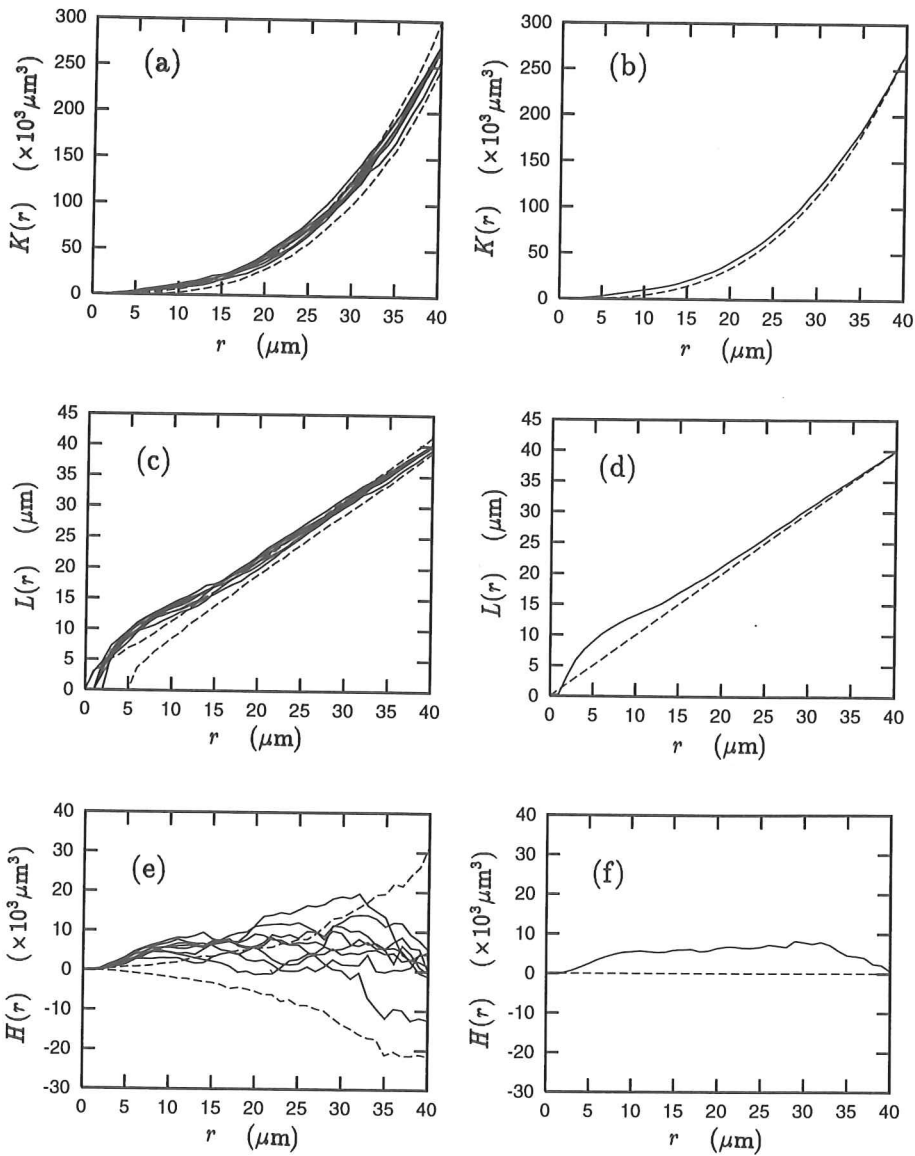


Figure 2: Results of the analysis of the pore centroid point pattern collected from eight bricks.—(a, c, and e) Individual estimates (solid lines) of $K(r)$, $L(r)$, and $H(r)$ together with lower and upper bounds (dashed lines) of the corresponding functions from 500 simulations of the Poisson reference model. (b, d, and e) Overall estimates (solid lines) of $K(r)$, $L(r)$, and $H(r)$ together with the corresponding theoretical Poisson reference models (dashed lines).

ACKNOWLEDGMENTS

We thank William P. Minnear, General Electric Company, Schenectady (USA) for providing the experimental material; Birgitta Christiansson, Ceramic Technology, the Royal Institute of Technology, Stockholm (Sweden) for preparing the specimen; and Olof Fransson, Physics IV, the Royal Institute of Technology, Stockholm (Sweden) for the original code to calculate centroids. L.M.K. acknowledges Sten Bergh and Per-Gunnar Rudolfsson, Norbergs Fastighets AB, Norberg (Sweden) for access to a room where L.M.K. worked while this work was carried out, and Trygghetsrådet (Sweden) for financial support.

REFERENCES

- Baddeley AJ, Howard CV, Boyde A, Reid S. Three-dimensional analysis of the spatial distribution of particles using the tandem-scanning reflected light microscope. In: Miles RE, ed. The commemorative-memorial volume. Twenty-five years of stereology. *Acta Stereol* 1987; 6/Suppl II: 87-100.
- Carlsson K, Liljeberg A. A confocal laser microscope scanner for digital recording of optical serial sections. *J Microsc* 1989; 153: 171-180.
- Diggle PJ. *Statistical Analysis of Spatial Point Patterns*. London: Academic Press, 1983.
- König D, Carvajal-Gonzales S, Down AM, Vassy J, Rigaut JP. Modelling and analysis of 3-D arrangements of particles by point processes with examples of application to biological data obtained by confocal scanning light microscopy. *J Microsc* 1991; 161: 405-433.
- Miles RE. The sampling, by quadrats, of planar aggregates. *J Microsc* 1978; 113: 257-267.
- Russ JC, Palmour III H, Hare TM. Direct 3-D pore location measurement in alumina. *J Microsc* 1989; 155: RP1-RP2.